# A Gated Liquid-Scintillator–Based Neutron Detector for Fast-Ignitor Experiments and Down-Scattered Neutron Measurements

## Introduction

Neutron detectors in inertial confinement fusion experiments are predominantly used to measure the neutron yield[1] and ion temperature[2] of the primary fusion reaction. These experiments produce nearly monoenergetic neutron spectra with energies of ~2.45 MeV for deuterium–deuterium (D–D) reactions and 14.1 MeV for deuterium–tritium (DT)–filled targets. The neutron spectra are broadened only slightly by the temperature of the core plasma,[2] which is of the order of a few keV. Neutron detectors are also utilized to detect secondary DT neutrons from targets filled with pure deuterium to infer the areal density of the fuel.[3] The secondary DT neutrons show a broad spectrum that depends on the fuel areal density, typically from 10 to 18 MeV, with a yield of the order of $10^{-3}$ of the primary neutrons. Since these secondary DT neutrons are faster than the primary DD neutrons, they can be easily detected with a time-resolved detector at a sufficient distance from the target to allow for neutron time-of-flight dispersion, which is of the order of ~25 ns/m. Even though the large background from the primary neutrons generally saturates the detector and recording system, this does not significantly affect the secondary neutron measurements because the secondary neutrons are recorded well before the background arrives. Recently, two new applications for neutron detectors have been proposed: (1) fast-ignition (FI) experiments with cone-in-shell targets[4] and (2) down-scattered neutron measurements in inertial fusion experiments,[5] which are much more challenging since they require the measurement of a small signal after a large background. In FI experiments the neutron spectrum of interest is quasi-monoenergetic, generally at ~2.45 MeV from D–D reactions. The background consists of hard x rays from the interaction of the high-energy short-pulse laser with the gold cones with an apparent spectral temperature of the order of ~1 MeV. The temporal dispersion between signal and background is high (~40 ns/m), but the background can easily be $10^5$ times higher than the signal. For the down-scattered neutron measurements, the background is the primary DT neutrons and the signal is the neutrons with energies below 12 MeV, typically 6 to 10 MeV. The signal-to-background ratio depends on the areal density of the target and is of the order of $10^{-2}$ for full-scale ignition targets. The temporal time-of-flight dispersion is small, approximately 4 ns/m for 10-MeV neutrons, compared to the primary 14.1-MeV DT neutrons. This article describes a current-mode neutron detector developed at LLE using a fast oxygen-enriched liquid scintillator coupled to a gated microchannel plate photomultiplier for FI and down-scattered neutron measurements.

## X-Ray Shielding

While shielding cannot be used for down-scattered neutron measurements to separate signal from background since there is no significant attenuation difference between 14.1-MeV and 6- to 12-MeV neutrons in any material, x-ray shielding has been used successfully to measure neutrons in high-energy short-pulse laser experiments at ~500-J laser energy and 1-ps pulse duration.[6] The detector described in Ref. 6 [an 18-cm-diam, 10-cm-thick Pilot B[7] scintillator, coupled to a conventional XP2020[8] photomultiplier tube (PMT)] was set up 2 m from the target for integrated FI experiments on the OMEGA Laser System.[9] Lead shielding with 15-cm thickness toward the target and 5 cm in all other directions was used to attenuate the hard x-ray background [see Fig. 123.37(a)]. The expected neutron yield from the FI experiments are of the order of $10^7$, which would produce a signal of ~1 V in the PMT. Figure 123.37(b) shows an example from a neutron-producing shot with a yield of $1.1 \times 10^7$ without the short-pulse laser firing. In an integrated FI experiment with a short-pulse laser energy of 1 kJ at 10 ps, the PMT is heavily saturated and no neutron signal is visible at all [Fig. 123.37(c)]. An additional factor of 1000 of x-ray attenuation is a rough estimate of what would be required to avoid saturation. The attenuation coefficients for Pb at photon energies of 2 to 10 MeV can be obtained from the NIST, XCOM[10] database to be ~4 to $5 \times 10^{-2}$ cm$^2$/g, which translates into a $1/e$ attenuation length of ~2 cm. Therefore an additional ~15 cm of Pb shielding would be required to avoid saturation. The total neutron-scattering cross section at 2.45 MeV is approximately 7 barn for Pb, according to the LBL, ENDF[11] database, which translates into a $1/e$ attenuation length of ~4 cm. Consequently, the neutron signal would also be attenuated by approximately

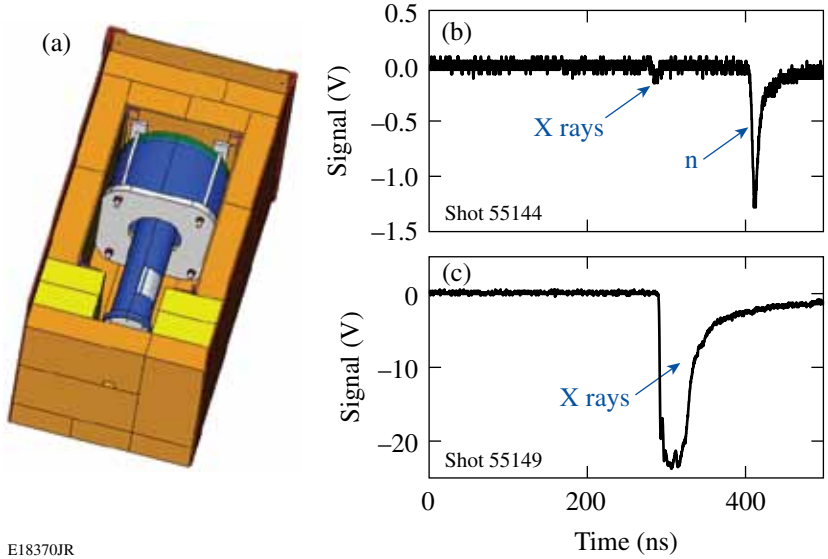


Figure 123.37
(a) CAD model of the detector shielding. (b) Neutron signal from a shot with a yield of $1.1 \times 10^7$. (c) X-ray background from a 1-kJ, 10-ps short pulse interacting with a fast-ignition target.

a factor of 50 and significantly broadened in time because of multiple scattering in the Pb shielding, making it almost impossible to detect.

**Photomultiplier Gating**

Another method to suppress the background signal, which works for both the FI experiments and the down-scattered neutron measurements, is to gate the PMT, rendering it inactive when the background signal is present. A PMT can be gated by applying a short positive pulse of the order of 200 V to the photocathode, which extracts the photoelectrons from the photocathode and prevents them from reaching the microchannel plate (see Fig. 123.38). A gated PMT240 from PHOTEK[12] was used in the NIF neutron time-of-flight (nTOF) detector, as described in Ref. 13, for FI experiments. The PMT was operated at a gain of $10^6$ coupled to a 40-mm-diam, 20-mm-thick BC422[14] plastic scintillator shielded with 25 mm of Pb. The detector was placed 5.2 m from the target. The gating pulse was set up to eliminate the hard x-ray pulse from the short-pulse interaction, which is recorded at ~350 ns (see Fig. 123.39). Up to an energy of ~500 J, the PMT gating reduces the pulse significantly, but at ~800 J of short-pulse energy the gating ceases to be effective and the PMT is saturated.

By removing the scintillator, it was verified that the background signal is produced predominantly by interactions with the microchannel plate (MCP). Since the MCP voltage is almost unchanged by the gate pulse, electrons generated inside the MCP will be amplified and a signal will be recorded, even if the gate voltage is applied. To avoid saturation from direct interaction with the MCP, a neutron detector was set up below the 60-cm-thick concrete floor below the target chamber at

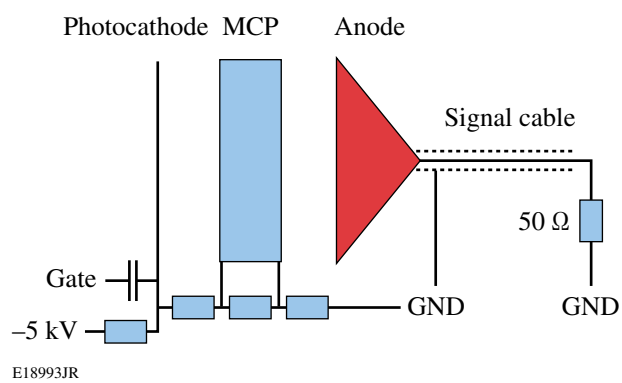


Figure 123.38
Simplified electrical schematic of the photomultiplier gating circuit. A resistive divider sets up the voltages between the photocathode, microchannel plate (MCP), and anode. A positive pulse at the gate input extracts the photoelectrons, disabling the photomultiplier tube (PMT).

12.4 m from the target [see Fig. 123.40(a)]. A 20-cm-diam hole in the floor provided an unshielded line of sight from the target to the detector. The gated PMT240 was mounted ~20 cm from the scintillator outside the direct line of sight through the hole. To compensate for the larger distance to target and the reduced light-collection efficiency, the scintillator size was increased to 18-cm diameter × 10-cm thickness.

A 2.5-cm-thick lead x-ray shield covering the hole in the floor eliminates the x-ray background with energies <1 MeV. In this configuration the PMT gating works well and the background is reduced to a very low level, as seen in Fig. 123.40(b). Unfortunately the light output from the plastic scintillator has a significant component with a long decay constant, which produces a strong background once the PMT gate ends. This

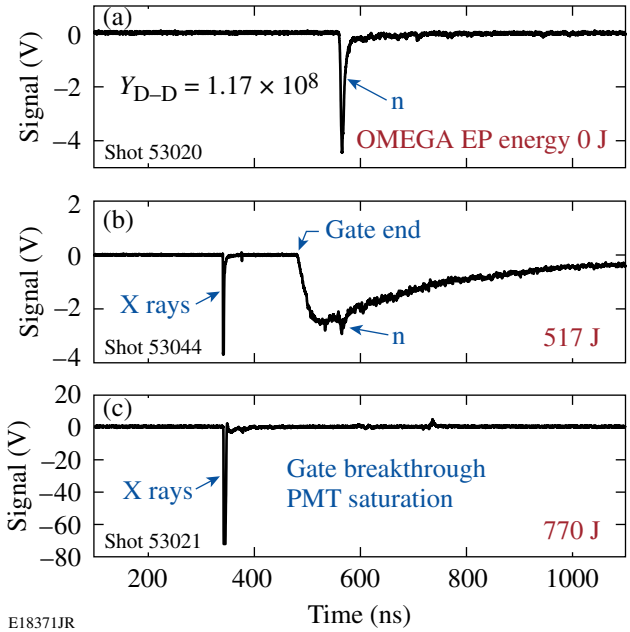


Figure 123.39
Signal from gated PMT in NIF nTOF detector: (a) no short pulse, (b) short-pulse energy of 517 J, and (c) short-pulse energy of 770 J.

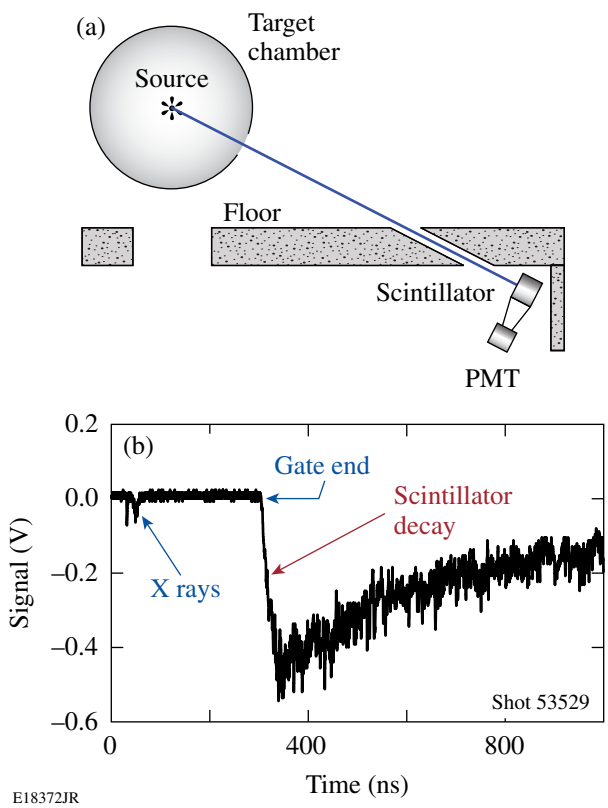


Figure 123.40
(a) Setup used to shield the PMT from direct hard x-ray irradiation; (b) signal from 1-kJ fast-ignition shot.

scintillator afterglow completely masks any neutron signal from D–D fusion reactions, which is expected to appear at ~550 ns, given the time-of-flight distance.

### Oxygen-Enriched Liquid Scintillator

To avoid background from the scintillator decay, a scintillator material with a significantly reduced long-decay component is required. Recently a low-afterglow liquid scintillator described in the literature showed a >100× decreased light output for times >100 ns after the primary event.[15] This liquid scintillator is based on a mixture of two dyes, PPO and bis-MSB, dissolved in xylene and enriched with molecular $O_2$. A neutron detector using this scintillator material was set up using the line of sight below the concrete floor shown in Fig. 123.40. It consists of a 3-L volume of oxygen-enriched liquid scintillator coupled to a gated PMT240 (see Fig. 123.41). A small air bubble allows for thermal expansion of the liquid without a significant pressure increase. The PMT is placed outside the direct line of sight to the target to avoid direct x-ray interactions with the MCP [see (Fig. 123.40)]. Data from integrated FI experiments with 1 kJ of short-pulse energy show a dramatically reduced scintillator decay tail and a very clear D–D neutron signal at the expected time [see Fig. 123.42(a)]. A very similar detector with a slightly smaller scintillator volume of ~1 L was fielded on high-areal-density cryogenic D–T implosions,[16] for down-scattered neutron measurements. The gating of the D–T primary peak works quite well, and the 2.45-MeV D–D fusion neutron peak is very well resolved [see Fig. 123.42(b)]. Unfortunately, a large background can still be seen in the signal after the gate turns off and the PMT becomes active. This background is predominantly caused by scattered primary DT neutrons that enter the room under the target area through

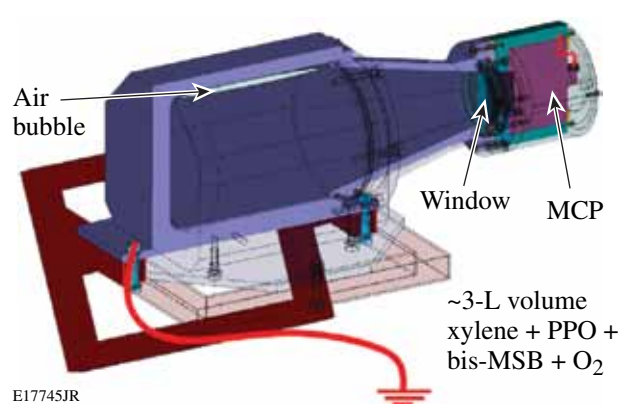


Figure 123.41
Drawing of the liquid scintillator detector.

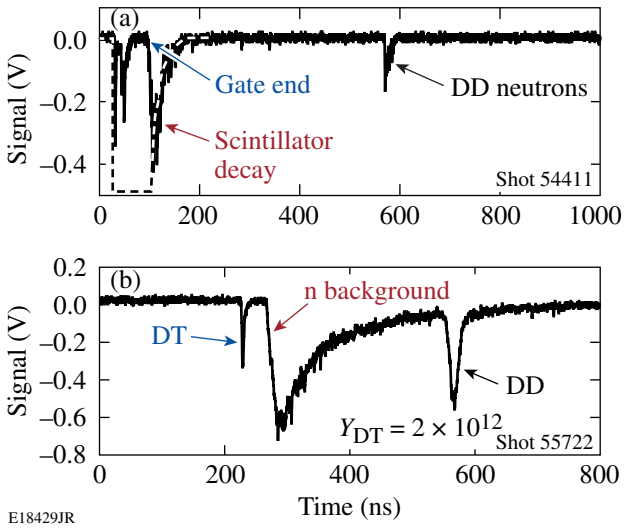


Figure 123.42
Signals recorded from the oxygen-enriched scintillator detector: (a) from FI experiments with 1 kJ of short-pulse energy and (b) high-areal-density cryogenic implosions.

a large hole under the target chamber and reach the detector through a large number of different pathways at different times. This was verified by blocking the direct line of sight to the target, resulting in a very similar background signal, without either the primary D–T or D–D peak.

## Summary and Conclusions

The detection of a small neutron signal after a very large background of hard x rays from short-pulse-laser–target interactions in a FI experiment or neutrons of higher energy in down-scattered neutron measurements is a very challenging task. Only the proper combination of sophisticated shielding, gating of a fast MCP-PMT, and a low-afterglow scintillator made it possible to record the D–D thermal neutron peak in integrated FI experiments at 1 kJ of short-pulse energy. In experiments with high-areal-density cryogenic DT targets, it was possible to clearly observe the D–D neutron peak, but the smaller down-scattered neutron signal is still masked by scattered primary neutrons that reach the detector because of insufficient neutron shielding. An improved neutron shielding for down-scattered neutron measurements on OMEGA is currently being designed and will be fielded in the near future.

## ACKNOWLEDGMENT

This work was supported by the U.S. Department of Energy Office of Inertial Confinement Fusion under Cooperative Agreement No. DE-FC52-08NA28302, the University of Rochester, and the New York State Energy Research and Development Authority. The support of DOE does not constitute an endorsement by DOE of the views expressed in this article.

## REFERENCES

1. M. D. Cable and M. B. Nelson, Rev. Sci. Instrum. **59**, 1738 (1988).
2. T. J. Murphy, R. E. Chrien, and K. A. Klare, Rev. Sci. Instrum. **68**, 610 (1997).
3. V. Yu. Glebov, D. D. Meyerhofer, C. Stoeckl, and J. D. Zuegel, Rev. Sci. Instrum. **72**, 824 (2001).
4. R. Kodama *et al.*, Nature **418**, 933 (2002).
5. V. Yu. Glebov, D. D. Meyerhofer, T. C. Sangster, C. Stoeckl, S. Roberts, C. A. Barrera, J. R. Celeste, C. J. Cerjan, L. S. Dauffy, D. C. Eder, R. L. Griffith, S. W. Haan, B. A. Hammel, S. P. Hatchett, N. Izumi, J. R. Kimbrough, J. A. Koch, O. L. Landen, R. A. Lerche, B. J. MacGowan, M. J. Moran, E. W. Ng, T. W. Phillips, P. M. Song, R. Tommasini, B. K. Young, S. E. Caldwell, G. P. Grim, S. C. Evans, J. M. Mack, T. Sedillo, M. D. Wilke, D. C. Wilson, C. S. Young, D. Casey, J. A. Frenje, C. K. Li, R. D. Petrasso, F. H. Séguin, J. L. Bourgade, L. Disdier, M. Houry, I. Lantuejoul, O. Landoas, G. A. Chandler, G. W. Cooper, R. J. Lepeer, R. E. Olson, C. L. Ruiz, M. A. Sweeney, S. P. Padalino, C. Horsfield, and B. A. Davis, Rev. Sci. Instrum. **77**, 10E715 (2006).
6. C. Stoeckl, V. Yu. Glebov, P. A. Jaanimagi, D. D. Meyerhofer, T. C. Sangster, M. Storm, S. Sublett, W. Theobald, M. H. Key, A. J. MacKinnon, P. Patel, P. A. Norreys, and D. Neely, Rev. Sci. Instrum. **77**, 10F506 (2006).
7. Nuclear Enterprises Ltd., Edinburgh, Midlothian EH11 4BY, United Kingdom.
8. Koninklijke Philips Electronics N.V., 1070 Amsterdam, The Netherlands.
9. C. Stoeckl, J. A. Delettrez, J. H. Kelly, T. J. Kessler, B. E. Kruschwitz, S. J. Loucks, R. L. McCrory, D. D. Meyerhofer, D. N. Maywar, S. F. B. Morse, J. Myatt, A. L. Rigatti, L. J. Waxer, J. D. Zuegel, and R. B. Stephens, Fusion Sci. Technol. **49**, 367 (2006).
10. Physics Laboratory, National Institute of Standards and Technology (NIST), http://www.nist.gov/physlab/index.cfm.
11. Experimental Nuclear Reaction Data (EXFOR/CSISRS), http://www.nndc.bnl.gov/exfor/.
12. Photek Ltd., St. Leonards-on-Sea, East Sussex, TN38 9NS, United Kingdom.
13. Z. A. Ali, V. Yu. Glebov, M. Cruz, T. Duffy, C. Stoeckl, S. Roberts, T. C. Sangster, R. Tommasini, A. Throop, M. Moran, L. Dauffy, and C. Horsefield, Rev. Sci. Instrum. **79**, 10E527 (2008).
14. Saint-Gobain Cristaux & Detecteurs, 38910 Gieres, France.
15. R. Lauck *et al.*, IEEE Trans. Nucl. Sci. **56**, 989 (2009).
16. V. N. Goncharov, T. C. Sangster, T. R. Boehly, S. X. Hu, I. V. Igumenshchev, F. J. Marshall, R. L. McCrory, D. D. Meyerhofer, P. B. Radha, W. Seka, S. Skupsky, C. Stoeckl, D. T. Casey, J. A. Frenje, and R. D. Petrasso, Phys. Rev. Lett. **104**, 165001 (2010).